

# Fine-Grained 3D Shape Classification with Hierarchical Part-View Attentions

Xinhai Liu, Zhizhong Han, Yu-Shen Liu, and Matthias Zwicker

**Abstract**—Fine-grained 3D shape classification is important and research challenging for shape understanding and analysis. However, due to the lack of fine-grained 3D shape benchmark, research on fine-grained 3D shape classification has rarely been explored. To address this issue, we first introduce a new dataset of fine-grained 3D shapes, which consists of three categories including airplane, car and chair. Each category consists of several subcategories at a fine-grained level. According to our experiments under this fine-grained dataset, we find that state-of-the-art methods are significantly limited by the small variance among subcategories in the same category. To resolve this problem, we further propose a novel fine-grained 3D shape classification method named FG3D-Net to capture the fine-grained local details of 3D shapes from multiple rendered views. Specifically, we first train a Region Proposal Network (RPN) to detect the generally semantic parts inside multiple views under the benchmark of generally semantic part detection. Then, we design a *hierarchical part-view attention aggregation* module to learn global shape representation by aggregating generally semantic part features, which preserves the local details of 3D shapes. The part-view attention module leverages a part-level attention and a view-level attention to increase the discriminative ability of features, where the part-level attention highlights the important parts in each view while the view-level attention highlights the discriminative views among all the views from the same object. In addition, we integrate the Recurrent Neural Network (RNN) to capture the spatial relationships among sequential views from different viewpoints. Our results under the fine-grained 3D shape dataset show that our method outperforms other state-of-the-art methods. The FG3D dataset is available at <https://drive.google.com/drive/folders/1zLDdE8mMlxVKh3usnUhqTwm-o9TbIMdV?usp=sharing>

**Index Terms**—Fine-Grained Shape Classification, 3D Objects, Generally Semantic Part, Dataset, Attention, Recurrent Neural Network.

## I. INTRODUCTION

LEARNING shape representation from multiple rendered views is an effective way to understand various 3D shapes [1], [2], [3], [4]. Influenced by the great success of Convolutional Neural Networks (CNNs) in the recognition of 2D images under large-scale datasets, such as ImageNet [5], 2D CNNs are intuitively applied to learn the representation for

X. Liu and Y.-S. Liu are with the School of Software, BNRist, Tsinghua University, Beijing 100084, China (e-mail: lxx17@mails.tsinghua.edu.cn, liuyushen@tsinghua.edu.cn)(Corresponding author: Yu-Shen Liu).

Z. Han is with the School of Software, Tsinghua University, Beijing 100084, China, and also with the Department of Computer Science, University of Maryland at College Park, College Park, MD 20737 USA (e-mail: h312h@mail.nwpu.edu.cn).

Matthias Zwicker is with the University of Maryland, College Park, 20737, USA (email: zwicker@cs.umd.edu).

This work was supported by National Key R&D Program of China (2018YFB0505400).

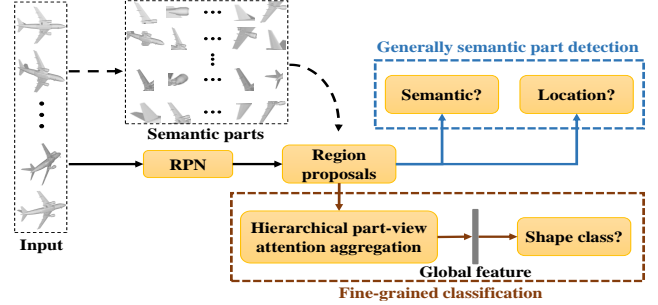


Fig. 1. The illustration of our FG3D-Net. In FG3D-Net, we first render each 3D shape into multiple views which are propagated into a Region Proposal Network (RPN) [6] to generate a set of region proposals. Then, the extracted region proposals are used in two different branches including generally semantic part detection (top branch in blue box) and fine-grained classification (bottom branch in brown). In the generally semantic part detection branch, we predict the semantic score and the bounding box location for each region proposal. And according to the semantic scores, several region proposals are selected to extract the global feature of the input 3D shape in the fine-grained classification branch. Specifically, we introduce a novel module named *hierarchical part-view attention aggregation* to effectively capture the fine-grained details of 3D shapes in fine-grained classification.

3D shapes. For example, the pioneer MVCNN [1] first projects a 3D shape into multiple views from different viewpoints and then obtains the global representation of the 3D shape by aggregating the view features with a view pooling layer, where the view features are extracted by a shared CNN. The previous view-based methods have achieved satisfactory performances in the recognition of 3D shapes with large variance among different categories. However, it is still nontrivial for these methods to capture the small variance among subcategories in the same category, which limits the discrimination of learned features in the fine-grained 3D shape recognition.

Fine-grained 3D shape recognition, which aims to discriminate 3D shapes within the same category, such as airliners, fighters and seaplanes from the category airplane, is quite challenging. Specifically, there are two major challenges which limit the development of fine-grained visual classification of 3D shapes. On the one hand, many large-scale image datasets (e.g. CUB-200-2011 [7] and Stanford dog dataset [8]) have been developed for fine-grained shape classification and recognition, but similar large-scale 3D object dataset is still lacking for fine-grained 3D shape classification. Recently, several well-known large-scale online 3D shape repositories, such as ShapeNet [9] and ModelNet [10], have been developed for learning shape representation in various applications, which contain various 3D objects from different categories, but these objects are not well organized for fine-grained 3D

shape classification. On the other hand, the existing view-based methods for learning 3D shape representation are not specially designed for more comprehensively capturing the fine-grained details from multiple views, especially for the fine-grained classification of 3D shapes. Intuitively, subtle and local differences are usually exposed in objects' parts, so it is vital to leverage the parts in fine-grained 3D shape classification.

Previous multi-view based methods [2], [1], [11] usually first extract a feature from pixel-level information in each view and then aggregate the extracted view features into a global shape representation. However, these methods can not capture part-level semantics from multiple views for 3D global feature learning. To address this problem, our recent work named Parts4Feature [12] utilized a region proposal network to detect generally semantic parts from multiple views and then learned to directly aggregate all generally semantic parts into a global shape representation. However, there are still several unresolved problems in Parts4Feature limiting its performances in the fine-grained classification of 3D shapes. Firstly, Parts4Feature can not capture the correlation of generally semantic parts in the same view, which makes it unable to filter out some meaningless generally semantic parts. Second, Parts4Feature ignores view-level information such as the importances of each view and the spatial relationship among sequential views, which is important for learning fine-grained 3D shape features. To solve the above-mentioned problems, we further propose a novel fine-grained 3D shape classification method, named FG3D-Net, as shown in Fig. 1, which leverages a hierarchical part-view attention aggregation module to capture the fine-grained features. Similar to [12], we first employ a region proposal neural network to detect generally semantic parts in each one of multiple views, which is considered to contain rich local details of 3D shapes. Then, to aggregate all these extracted generally semantic parts, we leverage semantic information at different levels including part-level, view-level and shape-level, respectively. Specifically, we introduce the part-level attention to highlight the important parts in each view and the view-level attention to highlight discriminative views among all the views of the same object. And benefited from the input setting of sequential views used in [13], we employ a Recurrent Neural Network (RNN) to encode the spatial relationship among views. In order to eliminate the impact of the initial view of RNN inputs, we integrate 3D shape global feature with a max-pooling operation as [1], which is invariant to the permutation of views.

Furthermore, we introduce a new fine-grained 3D shape dataset which contains three object categories including *Airplane*, *Car*, and *Chair*, where dozens of subcategories are constructed in each category. All 3D objects in the dataset are collected from several online repositories and are organized under the WordNet [14] taxonomy. Different from existing 3D datasets such as ShapeNet [9] and ModelNet [10], our 3D shape dataset is organized under fine-grained 3D shape classification benchmark, where each 3D object is strictly divided into one subcategory in a category. Our main contributions are summarized as follows.

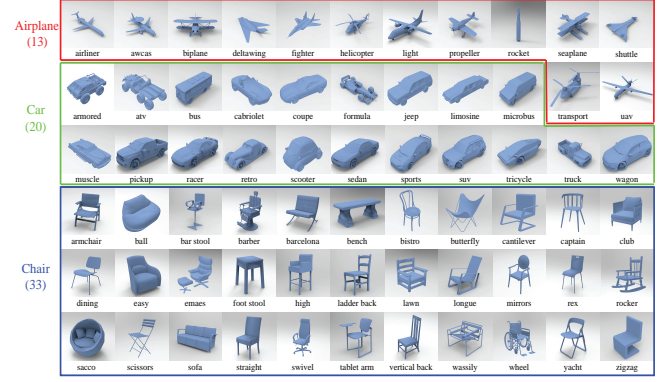


Fig. 2. There are three shape categories in our fine-grained dataset including *Airplane*, *Car* and *Chair*. Specifically, 13 shape subcategories are included in the *Airplane* category such as airliner, fighter and seaplane. In addition, 20 shape subcategories such as bus, jeep and scooter are involved in the *Car* category and the *Chair* category consists of 33 shape subcategories including bistro, captain, rocker, etc.

- We present a new fine-grained 3D shape dataset including three categories including *Airplane*, *Car* and *Chair*, which contains tens of thousands of 3D shapes and can be adopted as a benchmark for the task of fine-grained 3D shape classification.
- We propose a novel deep neural network named FG3D-Net to extract the global representation for 3D shapes, which captures the fine-grained local details from generally semantic parts to learn discriminative shape representations.
- We introduce part-level attention and view-level attention to highlight the more generally semantic parts in each view and the more distinctive views for each object, respectively.

## II. RELATED WORK

### A. 3D shape datasets

3D shapes are widely used in various applications, such as robotics [15] and 3D modeling [16]. In recent years, 3D shape understanding has attracted a lot of research interest. However, due to the inherent complexity of 3D shapes, 3D shape understanding is still a challenging problem in 3D computer vision. Benefiting from deep learning models, deep neural network based methods have achieved significant performances in the recognition of 3D shapes. These methods require large-scale 3D datasets which are important for training deep neural networks and evaluating the performances of algorithms. Researchers have been working on building many large-scale repositories [17], [18], [10], [19] which are widely adopted to evaluate deep neural networks in various applications. With the development of web-scale datasets, ShapeNet [9] has collected a large-scale synthetic 3D CAD models from online open-sourced 3D repositories, including more than three million models and three thousand object categories. Some other 3D repositories [20], [21], [22], [23] were also proposed, which contain semantic labels to the segmented components of 3D shapes. Recently, PartNet [24]

provided more fine-grained part annotations to support fine-grained level 3D shape segmentation tasks. However, there is still no suitable 3D shape benchmark for the fine-grained 3D shape classification task so far.

To address this problem, some previous studies introduced several fine-grained image datasets and evaluated the results of fine-grained 3D shape classification. FGVC-Aircraft [25] has collected ten thousand images of aircraft spanning 100 aircraft objects. And Car dataset [26] contains 16,185 images from 196 subcategories of car. Unfortunately, previous 3D fine-grained datasets usually represent the 3D shape with single 2D image, which can be regarded as the benchmarks of the fine-grained 2D image classification. Therefore, in FG3D-Net, we present a fine-grained 3D shape dataset containing 3D shapes represented by 3D meshes, where these shapes can be easily translated into other 3D data formats such as rendered views, point clouds and volumetric voxels. In Fig. 2, we show all the subcategories in our fine-grained datasets of three categories including airplanes, cars and chairs, respectively. The construction of the fine-grained dataset will be illustrated in Section III. FG3D DATASET. With the proposed fine-grained 3D shape dataset, we can evaluate the ability of algorithms in capturing shape details under fine-grained 3D shape classification.

### B. Fine-grained classification

Fine-grained classification aims to classify many subcategories under a same basic-level category such as different cats, dogs or cars. Due to the large intra-subcategory variance and the small inter-subcategory variance, fine-grained classification is a long standing problem in the computer vision. Recently, deep learning based methods have been widely applied to fine-grained image classification and achieved significant improvement over traditional methods. From the perspective of fine-grained image classification, current methods can be summarized into three categories: (1) ensemble of networks based methods, (2) visual attention based methods, (3) part detection based methods.

Firstly, ensemble of networks based methods were proposed to learn different representations of images for better classification performances with multiple neural networks. MGD [27] trained series of CNNs at multiple levels, which focuses on different region of interests in images. B-CNN [28] was proposed with a bilinear CNN model, which jointly combined two CNN feature extractors. Spatial Transformer [29] was proposed with a learnable model which consists of three parts including localization network, grid generator and sampler. The discriminative parts inside images were captured by four parallel spatial transformers on images and passed to the part description subnets.

Secondly, influenced by attention mechanism, researchers also focus on searching discriminative part dynamically, rather than dealing with images directly. AFGC [30] employed an attention mechanism for fine-grained classification system, which utilized the information of multi-resolution crops to obtain the location and the object on the input images.

Finally, subtle and local differences are usually shown in discriminative parts of object. Therefore, the discriminative

part detection is very important for the fine-grained shape classification. The R-CNN family approaches [6] employed a popular strategy which first generates thousands of candidate proposals and then filters out these proposals with confidence scores and bounding box locations. And [31] was proposed to detect discriminative parts for fine-grained image classification and trained a classifier on the features of detected parts. Recently, some studies [32], [33] focused on detecting discriminative parts under the weakly supervised setting, which means neither object nor part annotations are needed in both training and testing phases. In [32], part detectors were trained by finding constellations of neural activation patterns computed using convolutional neural networks. Specifically, the neural activation maps were computed as part detectors by using the outputs of a middle layer of CNN. All these methods have been proposed to accomplish fine-grained classification of 2D images. However, the fine-grained classification of 3D shapes is seldomly explored so far.

To resolve the above-mentioned issue, we propose FG3D-Net to learn fine-grained 3D global feature by capturing geometry details in generally semantic parts.

### C. Deep learning based methods for 3D shapes

Benefiting from the advances in deep learning, deep learning based methods have achieved significant performances in 3D shape understanding tasks such as shape classification and recognition. In general, current methods can be categorized into mesh based deep learning methods, voxel based deep learning methods, point clouds based deep learning methods and view based deep learning methods. To directly learn 3D features from 3D meshes, circle convolution [34] and mesh convolution [35] were proposed to learn local or global features from the geometry and spatial information on meshes to understand 3D shapes. Similar to images, voxels also have regular structure which can be learned by deep learning models, such as CRBM [36], fully convolutional denoising autoencoders [37], CNNs [38] and GAN [39]. These methods usually employ 3D convolution to better capture the contextual information inside local regions. Moreover, Tags2Parts [40] discovered semantic regions that strongly correlate with user-prescribed tags by learning from voxels using a novel U-Net. As a series of pioneering work, PointNet [41] and PointNet++ [42] inspired various supervised methods to understand point clouds. Through self-reconstruction, FoldingNet [43] and LatentGAN [44], [45], [46] learned global features with different unsupervised strategies. Similar to the light field descriptor (LFD), GIFT [2] measured the difference between two 3D shapes using their corresponding view feature sets. Moreover, pooling panorama views [47], [48] or rendered views [49], [4], [12] are more widely used to learn global features. Different improvements from camera trajectories [50], view aggregation [51], [13], [46], [52], pose estimation [3] have been presented. Parts4Feature [12] integrated Region Proposal Network (RPN) to detect generally semantic parts in multiple views and then aggregated global shape feature from these generally semantic parts. However, it is still hard for current methods to fully explore the fine-grained details of 3D shapes in the



TABLE I  
THE STATISTICS OF OUR FG3D DATASET WHICH CONSISTS OF 3 CATEGORIES AND 66 SUBCATEGORIES.

Subcategory	Train	Test	Total	Subcategory	Train	Test	Total	Subcategory	Train	Test	Total
airliner	955	100	<b>1055</b>	muscle	468	100	<b>568</b>	dining	614	100	<b>714</b>
awcas	24	10	<b>34</b>	pickup	201	50	<b>251</b>	easy	990	100	<b>1090</b>
biplane	127	50	<b>177</b>	racer	383	100	<b>483</b>	emaes	73	40	<b>113</b>
deltawing	186	50	<b>236</b>	retro	102	50	<b>152</b>	foot stool	186	50	<b>236</b>
fighter	545	100	<b>645</b>	scooter	25	5	<b>30</b>	high	256	100	<b>356</b>
helicopter	549	100	<b>649</b>	sedan	2027	100	<b>2127</b>	ladder back	241	50	<b>291</b>
light	101	30	<b>131</b>	sports	427	100	<b>527</b>	lawn	84	30	<b>114</b>
propeller	288	100	<b>388</b>	suv	209	100	<b>309</b>	longue	665	100	<b>765</b>
rocket	390	100	<b>490</b>	tricycle	14	5	<b>19</b>	morris	154	50	<b>204</b>
seaplane	35	20	<b>55</b>	truck	131	50	<b>181</b>	rex	407	100	<b>507</b>
shuttle	201	50	<b>251</b>	wagon	427	100	<b>527</b>	rocker	121	50	<b>171</b>
transport	15	7	<b>22</b>	<b>Car total</b>	<b>7010</b>	<b>1315</b>	<b>8325</b>	sacco	114	50	<b>164</b>
uav	25	15	<b>40</b>	armchair	1578	100	<b>1678</b>	scissors	65	20	<b>85</b>
<b>Airplane total</b>	<b>3441</b>	<b>732</b>	<b>4173</b>	ball	226	100	<b>326</b>	sofa	307	100	<b>407</b>
armored	16	5	<b>21</b>	bar	606	100	<b>706</b>	straight	1553	100	<b>1653</b>
atv	77	30	<b>107</b>	barber	20	5	<b>25</b>	swivel	777	100	<b>877</b>
bus	936	100	<b>1036</b>	barcelona	35	10	<b>45</b>	tablet armed	51	20	<b>71</b>
cabriolet	477	100	<b>577</b>	bench	41	20	<b>61</b>	vertical back	748	100	<b>848</b>
coupe	528	100	<b>628</b>	bistro	48	20	<b>68</b>	wassily	18	5	<b>23</b>
formula	62	20	<b>82</b>	butterfly	10	5	<b>15</b>	wheel	7	5	<b>12</b>
jeep	276	100	<b>376</b>	cantilever	310	100	<b>410</b>	yacht	55	20	<b>75</b>
limousine	109	50	<b>159</b>	captain	217	50	<b>267</b>	zigzag	89	30	<b>119</b>
microbus	115	50	<b>165</b>	club	458	100	<b>558</b>	<b>Chair total</b>	<b>11124</b>	<b>1930</b>	<b>13054</b>

TABLE II  
THE DATASET COMPARISON BETWEEN OUR FG3D AND SHAPENET.

Category	#Subcategories	#Overlap Subcategories	#Total Shapes	#Overlap Shapes
Airplane (FG3D)	13	7	4173	3064
Airplane (ShapeNet)	11		4045	
Car (FG3D)	20	6	8235	3593
Car (ShapeNet)	18		4472	
Chair (FG3D)	33	20	13054	6781
Chair (ShapeNet)	23		8591	

fine-grained classification task. In FG3D-Net, we introduce a hierarchical part-view attention aggregation strategy to extract more discriminative information from generally semantic parts.

### III. FG3D DATASET

To evaluate the performance in fine-grained 3D shape classification, we introduce a fine-grained 3D shape (FG3D) dataset. Different from previous datasets such as ShapeNet [1], our FG3D dataset aims to evaluate the recognition results within the same shape category, where 3D shapes are with large intra-subcategory variance and small inter-subcategory variance.

Specifically, our FG3D dataset includes three shape categories, i.e., *Airplane*, *Car* and *Chair* with 3,441, 8,235 and 13,054 3D shapes, respectively. We represent each 3D shape by an object format file (.off) with the polygonal surface geometry. One can easily convert the .off files into other shape representations, such as rendered views, voxels and point clouds. All shapes in our FG3D dataset are collected from multiple online repositories including 3D Warehouse [53], Yobi3D [54] and ShapeNet [9], which contain a massive collection of CAD shapes that are publicly available for research purpose. By collecting 3D shapes over a period of two months, we finally obtain a collection of more than 20K 3D shapes in three shape categories. And these 3D shapes are organized under WordNet [14] noun “synsets” (synonym

sets). WordNet provides a broad and deep taxonomy with over 80K distinct synsets representing distinct noun concepts. This taxonomy has been utilized by ImageNet [5] and ShapeNet [9] to formulate the object subcategories. In our dataset, we also introduce the taxonomy into the collection of 3D shapes, as shown in Fig. 2.

For a good dataset, there are six crucial properties that are needed in fine-grained 3D shape classification [19], [24]: (1) large shape number which is important for deep networks to capture statistically significant patterns; (2) ground truth labels which enable to quantitatively evaluate the performance of learning in a specific task; (3) fine-grained requirement which contains dozens of subcategories under the same basic shape category; (4) typical representation that is convenient to be adopted as input; (5) 3D file format which deals with the challenges of 3D shape recognition; (6) expandable property which should be easy to make the collection grow over time, to keep the dataset challenging as progress of learning algorithms. To build the FG3D dataset, we collect large quantity of 3D shape files and classify each 3D shape into one unique subcategory, which strictly follows the above requirements.

Existing datasets are usually composed of 3D shapes from different basic categories such as ShapeNet [9] and ModelNet [36], but they do not satisfy the aforementioned property (3). Although there are also multiple subcategories under a basic category in ShapeNet, some 3D shapes with multiple



subcategory labels or incorrect subcategory labels make it hard to be used for fine-grained 3D shape classification. In addition, the image-based datasets such as FGVC-Aircraft [25] and Car dataset [26] do not satisfy the property (5), since there is no 3D shapes in the datasets. To resolve these issues, we propose a new dataset FG3D containing 3D shapes, which is complementary of current datasets and satisfies the properties (1)-(6). From the perspective of fine-grained visual classification, there are a considerable variation in the same subcategory and a slight variation among different subcategories under each shape category in the dataset.

As shown in TABLE I, the FG3D dataset consists of three categories including *Airplane*, *Car* and *Chair*, which contain 13, 20 and 33 object subcategories, respectively. For evaluation, we split the shapes in each categories into training sets and testing sets. Specifically, the 3D shapes in airplane are split into 3,441 for training and 732 for testing. The category of cars contains 7,010 shapes for training and 1,315 shapes for testing. And the category of chairs contains 11,124 shapes for training and 1,930 shapes for testing. Different from previous 3D object datasets such as ShapeNet [9] and ModelNet [36], our FG3D dataset is designed for fine-grained 3D shape classification. Previous ShapeNet also contains several subcategories in each categories. However, there are some misclassified 3D objects in the subcategories and repeated 3D objects among different subcategories. To solve above problems, we introduce our FG3D dataset to evaluate algorithms in the fine-grained 3D classification. And to show the differences with ShapeNet, we compare the details of FG3D dataset with the ShapeNet in these categories in TABLE II. From the comparisons, FG3D dataset contains more 3D objects and subcategories to support the fine-grained classification task.

#### IV. FG3D-NET

##### A. Overview

The framework of FG3D-Net is illustrated in Fig. 3, which consists of five modules including (a) sequential view capturing, (b) region proposal generation, (c) generally semantic part detection, (d) hierarchical part-view attention aggregation and (e) fine-grained classification, respectively. In particular, the modules (b) and (c) are known as a region proposal network and cooperate to finish the detection of Generally Semantic Parts (GSPs) from multiple rendered views, which are pre-trained under several part segmentation benchmarks. In the construction of region proposal network, we follow the similar strategy used in Parts4Feature [12] to detect the GSPs inside multiple views.

For each input 3D shape  $m$  in the training set, a view sequence  $v$  is first obtained by capturing  $V$  views  $\{v_i\}$  around  $m$ , such that  $v = [v_1, \dots, v_i, \dots, v_V]$  and  $i \in [1, V]$ , as shown in the module (a) of Fig. 3. Then, a shared convolution neural network (e.g., VGG19 [55]) abstracts all the views into feature maps in a high-dimensional space. By using a sliding window on the feature maps, numerous region proposals  $\{r_i^j\}$  are calculated for each view  $v_i$ , where the corresponding proposal features  $\{c_i^j\}$  are extracted by a RoI (Region-of-Interest) pooling layer and  $j \in [1, N]$ . With proposal features

$c_i^j$ , module (c) learns to predict both the semantic scores and bounding box locations of GSPs within multiple views. Finally, according to semantic scores, the features  $\{c_i^k\}$  of the top  $K$  region proposals  $\{r_i^k\}$  in each view  $v_i$  of  $v$  are selected to extract the global shape feature  $f$  of  $m$  with the module (d). The global shape feature  $f$  is propagated through a Fully Connected (FC) layer to provide the classification probability  $p$  in the benchmark of fine-grained 3D shape classification.

##### B. Generally semantic parts (GSPs)

The generally semantic part in FG3D-Net indicates a local part of any semantic part class in any shape category inside the views of 3D shapes, such as the wings of airplanes and the wheels of cars extracted from the views. Different from the semantic part in 3D shape segmentation, the generally semantic part of FG3D-Net represents local visual parts within 2D views rather than shape parts in the 3D space. By learning the shape representation using GSPs, our method is allowed to exploit the fine-grained details of multiple views in three levels including part-level, view-level and shape-level.

In the pre-training stage of GSPs detection, all training ground-truth GSPs are generated from several 3D shape segmentation benchmarks. By learning the GSPs from other 3D segmentation datasets, we are able to detect the GSPs in multiple views under our fine-grained classification benchmark without any ground-truth GSP supervision. Specifically, we use three 3D shape segmentation benchmarks including ShapeNetCore [56], Labeled-PSB [57], [22], and COSEG [57] to construct the generally semantic part detection benchmark and provide ground-truth GSPs. Here, we follow [58] to split the 3D shapes into training set and testing set.

Fig. 4 shows the generation pipeline of the ground-truth bounding boxes for GSPs. Based on the segmentation ground-truth in the 3D space, we can represent each segmented 3D part with different colors. To extract the bounding box for each 3D part, we render each colored 3D part into 2D images. And with an image processing step, a region property measurement function is applied to provide the bounding box for the colored parts. To decline the impact of data noise, we also apply data cleaning steps to eliminate influence of some small parts whose bounding boxes are smaller than 0.45 of the max bounding box in the same part category. In addition, the setting of GSPs can also eliminate the impact of some incorrect segmentations, where some 3D parts may have wrong part labels. So far, we have obtained the bounding boxes of the ground truth GSPs within multiple views, where the ground-truth GSPs are applied to train modules (b) and (c) for generally semantic part detection, as shown in Fig. 3.

##### C. Region proposal network

A Region Proposal Network (RPN) takes an image as input and outputs a set of rectangular object proposals, each with an objectness score. For FG3D-Net in Fig. 3, modules (a) and (b) are considered as one RPN together, which is modified to detect the GSPs in the multiple views of 3D shapes. Similar to [6], a set of generally semantic part proposals are detected from multiple views of 3D shapes. Specifically, in

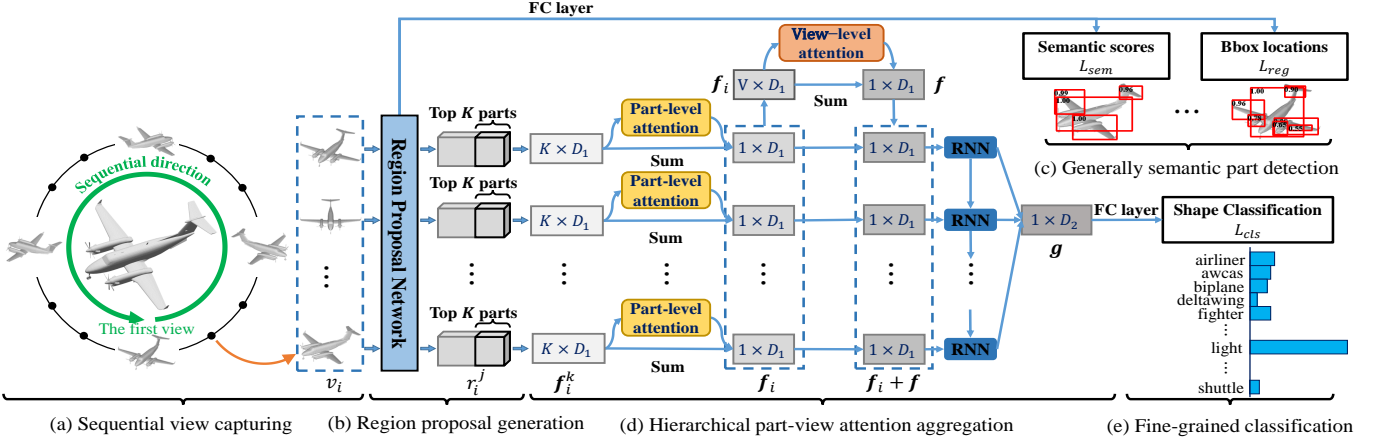


Fig. 3. The framework of FG3D-Net. A sequence of views are first rendered from multiple viewpoints around the input 3D shape in the sequential view capturing module (a). And all the views are propagated into a region proposal network to generate region proposals and to compute the corresponding proposal features with RoI pooling operation in module (b). Therefore, generally semantic parts in each view can be detected by predicting the semantic scores and bounding box (bbox) locations with several FC layers in the module (c). Then, according to the semantic scores, top  $K$  region proposals are selected to extract the global feature for input 3D shape in the hierarchically part-view attention aggregation module (d). There are three different semantic levels in the feature aggregation including part-level, view-level and shape-level. And two bilinear attention mechanisms are integrated to explore the correlation among features in different semantic levels. In addition, a RNN layer is applied to enhance the correlation of view features by taking advantage of the sequential views. Finally, the global shape representation is extracted by a max-pooling layer, which is applied to the fine-grained classification of 3D shapes in the module (e).

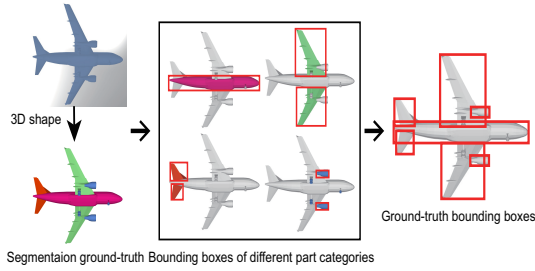


Fig. 4. The generation of ground-truth generally semantic parts from segmentation. According to the segmentation ground-truths, we first individually render each 3D part into 2D views with different colors. Then, we extract the bounding boxes of the colored parts using image processing. Finally, we obtain the ground-truth bounding-boxes of each 3D part in the 2D views.

the region proposal generation module (b), a lot of region proposal candidates  $\{r_i^j\}$  are generated in each view  $v_i$  and the corresponding proposal features  $\{c_i^j\}$  are also calculated by a Region-of-Interest (RoI) pooling layer. Then, in the generally semantic part detection module (c), all proposal features  $\{c_i^j\}$  are applied to predict both the semantic scores and locations of GSPs with several Fully Connected (FC) layers. According to the predicted semantic scores, the features  $\{c_i^j\}$  of top  $K$  proposals are forwarded to hierarchically learn 3D shape representations in the module (d). In module (b), there are a Convolutional Neural Network (CNN) layer, a region proposal calculation layer and a RoI pooling layer.

Firstly, the Convolutional Neural Network (CNN) abstracts the input multiple views into the feature maps. The CNN layer is modified from a VGG-19 network proposed in [55], and it produces a feature map  $c_i$  for each view  $v_i$  with a size of  $12 \times 12 \times 512$ . Secondly, a region proposal layer calculates region proposals  $\{r_i^j\}$  by sliding a small window on the corresponding feature map  $c_i$ . At each sliding-window location which is centered at each pixel of  $c_i$ , a region  $r_i^j$  is

proposed by regressing its location  $t_D$  and predicting semantic probability  $p_D$  with an anchor. The location  $t_D$  is a four dimensional vector representing center coordinates, width and height of the part bounding box. We also use 6 scales and 3 aspect ratios to yield  $6 \times 3 = 18$  anchors, which ensures a wide range of sizes to accommodate region proposals for GSPs that may be partially occluded in some views. The 6 scales relative to the size of the views are  $[1, 2, 4, 8, 16, 32]$ , and the 3 aspect ratios are  $1:1$ ,  $1:2$ , and  $2:1$ . Altogether, this leads to  $N = 2592 = 12 \times 12 \times 18$  regions  $\{r_i^j\}$  in each view  $v_i$ . All of the above modifications are derived from the Faster-RCNN [59].

To train RPN to predict the semantic scores  $p_D$  of GSPs, we assign a binary label to each region proposal  $r_i^j$  to indicate whether  $r_i^j$  is a GSP. Specifically, we assign a positive label if the IoU (Intersection-over-Union) overlap between  $r_i^j$  and any ground-truth GSP in  $v_i$  is higher than a threshold  $S_D$ . Note that a single ground-truth box may assign positive labels to multiple anchors; otherwise, we use a negative label. In each view  $v_i$ , we apply RoI pooling over region proposal location  $t_D$  on feature maps  $c_i$ . Hence, the features  $\{c_i^j\}$  of all  $N$  region proposals  $\{r_i^j\}$  are  $512 \times 7 \times 7$  dimensional vectors, which we forward to generally semantic part detection in Fig. 3 (c). To reduce the computing consumption, we represent each generally semantic part feature in the top  $K$  proposals with a 512-dimensional feature vector  $f_i^k$  which is calculated by  $f_i^k = \text{MAX}(\{c_i^j\})$ . Therefore, we finally obtain the features  $\{f_i^k\}$  of the top  $K$  region proposals  $\{r_i^j\}$  according to their semantic scores  $p_D$ , which are propagated to the hierarchical part-view attention aggregation module in Fig. 3 (d).

With the above definitions, an objective function is employed to optimize the part detection following the multi-task loss in Faster-RCNN [6]. Denote that the ground-truth semantic scores and box locations of positive and negative

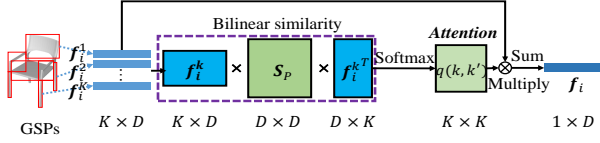


Fig. 5. The demonstration of part-level attention. By calculating the attention values among generally semantic parts, we aggregate  $K$  parts features  $\{f_i^k\}$  in the same view into a view feature  $f_i$ . Firstly, we compute the bilinear similarity score  $q(k, k')$  between  $f_i^k$  and  $f_i^{k'}$  with a softmax layer. Then, we multiply the scores  $q(k, k')$  to the input part features to highlight the discriminative features. Here,  $\otimes$  indicates the multiply operation. Finally, a weighted sum operation is applied to aggregate the highlighted parts features into a view feature  $f_i$ .

samples in the RPN are  $p^*$  and  $t^*$ , respectively. The loss function is defined as

$$L(p_D, p^*, t_D, t^*) = L_{sem}(p_D, p^*) + \lambda L_{reg}(t_D, t^*), \quad (1)$$

where  $L_{sem}$  measures the accuracy in terms of semantic scores by the cross-entropy function of positive labels, while  $L_{reg}$  measures the accuracy of location in terms of the  $L_1$  distance [6]. The parameter  $\lambda$  balances the  $L_{sem}$  and  $L_{reg}$  in the training process. In the experiment,  $\lambda$  works well with a value of 1. By introducing the architecture of RPN [6], FG3D-Net has the powerful ability to detect GSPs from multiple views by learning under segmentation benchmarks.

#### D. Hierarchical part-view attention aggregation

In Fig. 3, the hierarchical part-view attention aggregation module (d) is the key component of FG3D-Net, which hierarchically learns the global representation  $f$  of the input 3D shape from generally semantic part features  $\{f_i^k\}$ . To aggregate features from low-level to high-level, it is important to preserve the detailed information in different levels. Thus, in module (d), there are three different levels including part-level, view-level and shape-level. Similarly, the local details of views also play a key role in the fine-grained classification of 3D shapes. To aggregate the features between different levels, three special designs are introduced including part-level attention, view feature enhancement and view-level attention.

1) *Part-level attention*: The target of part-level attention is to aggregate the features of GSPs detected in the same view. As shown in Fig. 5, we first select the top  $K$  GSP features  $\{f_i^k\}$  of view  $v_i$  that should be integrated into a view feature  $f_i$ . The traditional approaches [1] usually aggregate multiple features by max-pooling or mean-pooling operations. However, simple pooling operations lose a lot of content information within generally semantic part features. As summarized by some previous methods [60], [61], [62], [63] in the fine-grained classification of 2D images, the detail information of local parts usually determines the discriminativeness of learned object features. To resolve this issue, we propose the bilinear similarity attention to aggregate generally semantic part features  $\{f_i^k\}$  into view feature  $f_i$  for view  $v_i$  in the view sequence  $v$ . The part-level attention motivates to take advantage of the relationships among part features to facilitate

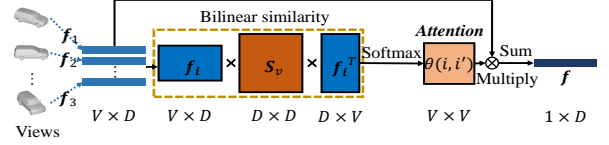


Fig. 6. The demonstration of view-level attention. Similar to the part-level attention, we calculate the bilinear similarity scores  $\theta(i, i')$  among the view features from the same 3D object to aggregate view features  $\{f_i\}$  into a shape feature  $f$ . By applying a multiply operation  $\otimes$  and a weighted sum operation, the global feature  $f$  is obtained with considering the importances of view features.

the feature aggregation procedure. Specifically, a shared matrix  $S_p$  is learned to evaluate the mutual correlations among the  $K$  generally semantic part features  $\{f_i^k\}$  of view  $v_i$ . Here the learnable matrix  $S_p$  is shared across all views, which aims to capture the general patterns among GSPs in each one of multiple views. In addition, the learning of  $S_p$  can also explore the generally semantic part feature patterns of 3D shapes from different subcategories. By applying an attention value to each GSP, the part-level attention can highlight the important and meaningful of GSPs in each view to facilitate the feature aggregation.

Given the GSP features  $\{f_i^k\}$  of view  $v_i$ , the corresponding context of  $f_i^k$  is formed by

$$R_{i,k}^{context} = \{f_i^k\}, k \in [1, K]. \quad (2)$$

For each candidate  $f_i^k$ , there is a score  $q(k, k')$  measuring the similarity between  $f_i^k$  and  $f_i^{k'}$  as follows

$$q(k, k') = \frac{\exp(f_i^k S_p f_i^{k'}{}^T)}{\sum_{n=1}^K \exp(f_i^k S_p f_i^n{}^T)}, \quad (3)$$

where  $S_p$  is the learnable matrix with a size of  $512 \times 512$ . All  $q_k$  form the bilinear similarity attention matrix with a size of  $K \times K$ , which represents the correlation among the  $K$  GSPs. Without extra selection of highly related ones, the context  $e_i^k$  fused for  $f_i^k$  is a weighted average over all the candidate parts, as denoted by

$$e_i^k = \sum_{k'=1}^K q(k, k') f_i^{k'}. \quad (4)$$

With the context vector of GSPs in view  $v_i$ , the view feature  $f_i$  can be calculated by

$$f_i = \sum_{k=1}^K e_i^k, \quad (5)$$

where the view features  $\{f_i\}$  are then propagated to the view feature enhancement module.

2) *View-level attention*: In the view-level, we can apply similar strategy to effectively aggregate view features  $f_i$  into 3D global features  $f$ , as depicted in Fig. 6, which contains the global information of a whole 3D shape from multiple views. To learn the attention of view features from the same 3D object, another learnable parameter matrix  $S_v$  is applied to capture the correlation among views. The attention value between each two view features is learned by calculating the



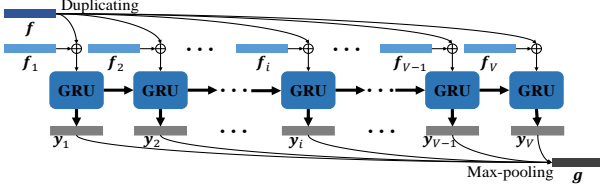


Fig. 7. The demonstration of the view feature enhancement. To enhance the view features, we first add the global shape feature  $\mathbf{f}$  to  $\mathbf{f}_i$  by duplicating, where  $\oplus$  indicates the sum operation. Then, we adopt a GRU (RNN) to capture the spatial correlation among views. Therefore, we obtain the enhanced view features  $\{\mathbf{y}_i\}$  which are aggregated into the final global shape representation  $\mathbf{g}$  by a max-pooling layer.

bilinear similarity, which can leverage the importance of views in the feature aggregation.

Given the view features  $\{\mathbf{f}_1, \mathbf{f}_2, \dots, \mathbf{f}_i, \dots, \mathbf{f}_V\}$ , a similarity score  $\theta(i, i')$  measuring the similarity between  $\mathbf{f}_i$  and  $\mathbf{f}_{i'}$  is computed as

$$\theta(i, i') = \frac{\exp(\mathbf{f}_i \mathbf{S}_v \mathbf{f}_{i'}^T)}{\sum_{l=1}^V \exp(\mathbf{f}_i \mathbf{S}_v \mathbf{f}_l^T)}, \quad (6)$$

where  $\mathbf{S}_v$  is also a learnable matrix with a size  $512 \times 512$  to capture the correlation among views. The all learned  $\theta(i, i')$  are the bilinear similarity attention matrix with a size of  $V \times V$ . And according to the learned similarity scores, the context  $\bar{\mathbf{e}}_i$  of view  $v_i$  is fused from  $\mathbf{f}_i$  with a weighted average over the views

$$\bar{\mathbf{e}}_i = \sum_{i'=1}^V \theta(i, i') \mathbf{f}_{i'}. \quad (7)$$

And the 3D global feature  $\mathbf{f}$  is computed as

$$\mathbf{f} = \sum_{i=1}^V \bar{\mathbf{e}}_i. \quad (8)$$

Through the hierarchical part-view attentions, we obtain the global shape representation  $\mathbf{f}$ , which can be applied to do recognition of 3D shapes. However, the spatial correlation among sequential views is not fully explored. To take advantage of the prior information of the view sequence  $\mathbf{v}$ , we additionally utilize recurrent neural network to enhance the 3D global feature  $\mathbf{f}$ .

3) *View feature enhancement*: An important prior information of sequential input views  $\mathbf{v}$  is the spatial information among them, where the rendering viewpoints are continuously distributed around the shape in the 3D space. To benefit from the powerful ability of learning from sequential data, FG3D-Net employs a Recurrent Neural Network (RNN) to learn the enhanced view features  $\{\mathbf{y}_i\}$  from the view features  $\{\mathbf{f}_i\}$  and the global feature  $\mathbf{f}$ .

With the view features  $\{\mathbf{f}_1, \mathbf{f}_2, \dots, \mathbf{f}_i, \dots, \mathbf{f}_V\}$  aggregated from the part level, we first integrate the information of global shape information by

$$\mathbf{f}'_i = \mathbf{f}_i + \mathbf{f}. \quad (9)$$

The integrated features  $\mathbf{f}'_i$  form a feature sequence  $\mathbf{f}'_v = \{\mathbf{f}'_1, \mathbf{f}'_2, \dots, \mathbf{f}'_i, \dots, \mathbf{f}'_V\}$ . A RNN takes the sequential view features as input and captures the spatial correlation among

views. The RNN consists of a hidden state  $\mathbf{h}$  and an optional output  $\mathbf{f}$ , which operates on the view feature sequence  $\mathbf{f}'_v$ . Here each item  $\mathbf{f}'_i$  is a 512-dimensional feature vector and the length of  $\mathbf{f}'_v$  is  $V$  which is also the step of RNN. At each time step  $t \in [1, V]$ , the hidden state  $\mathbf{h}_t$  of the RNN is updated by

$$\mathbf{h}_t = \text{GRU}(\mathbf{h}_{t-1}, \mathbf{f}'_t), \quad (10)$$

where  $\text{GRU}$  is a non-linear activation function named gated recurrent unit [64].

A RNN can learn the probability distribution over a sequence by being trained to predict the next item in the sequence. Similarly, at time step  $t$ , the output  $\mathbf{y}_t$  of the RNN can be represented as

$$\mathbf{y}_t = \mathbf{W}_a \mathbf{h}_t, \quad (11)$$

where  $\mathbf{W}_a$  is a learnable weight matrix. After forwarding the entire input feature sequence, as shown in Fig. 3, the output sequence  $\{\mathbf{y}_1, \mathbf{y}_2, \dots, \mathbf{y}_i, \dots, \mathbf{y}_V\}$  is acquired, which contains the content information and the spatial information of the entire view feature sequence. To avoid the impact of the initial input view feature of RNN, we adopt a max-pooling layer to learn more general global shape feature  $\mathbf{g}$  by

$$\mathbf{g} = \max_{i \in [1, V]} \{\mathbf{y}_i\}. \quad (12)$$

Through the view feature enhancement, a global representation  $\mathbf{g}$  is extracted from GSPs in multiple views. Following by a FC layer,  $\mathbf{g}$  is applied to predict 3D shape labels with the cross-entropy loss function, where the softmax function outputs the classification probabilities  $\mathbf{p}$ . Suppose that there are  $C$  shape subcategories of a same category in the classification, so each probability  $\mathbf{p}(c)$  can be defined as

$$\mathbf{p}(c) = \frac{\exp(\mathbf{W}_c \mathbf{g} + a_c)}{\sum_{c' \in [1, C]} \exp(\mathbf{W}_{c'} \mathbf{g} + a_{c'})}, \quad (13)$$

where  $\mathbf{W}$  and  $a$  are the weights of the FC layer to be learned. The objective loss function is the cross-entropy between the predicted probability  $\mathbf{p}$  and the corresponding ground truth  $\mathbf{p}'$ ,

$$L(\mathbf{p}, \mathbf{p}') = - \sum_{c \in [1, C]} \mathbf{p}'(c) \log(\mathbf{p}(c)). \quad (14)$$

### E. Training

There are two different tasks in our FG3D-Net including generally semantic part detection and fine-grained classification. To leverage the performances of the two tasks, we use an alternately training strategy to train the FG3D-Net. Firstly, we train the region proposal network to detect generally semantic parts inside shape views under the processed segmentation benchmarks. Then, with fixing the parameters in the region proposal network, we only update parameters inside the hierarchical part-view attention aggregation branch, as shown in Fig. 1. By repeating the above two steps, we can apply our FG3D-Net to extract discriminative shape features for 3D shapes in the fine-grained 3D shape classification. Therefore, the optimization target  $L_{total}$  of FG3D-Net consists of two parts, which is calculated as

$$L_{total} = L(p_D, p^*, t_D, t^*) + \psi L(\mathbf{p}, \mathbf{p}'). \quad (15)$$

Here,  $\psi$  is set to a value of 1 in the experiments.

## V. EXPERIMENTS

In this section, we conduct comprehensive experiments to validate FG3D-Net in the fine-grained visual classification of 3D shapes. We first present some statistics of the FG3D dataset which is proposed for the fine-grained 3D classification. Then, we explore how some key parameters affect the performance of our FG3D-Net. Finally, under our FD3D dataset, we compare the performances of our FG3D-Net with some state-of-the-art methods with different 3D shape representations.

### A. Network configuration

In FG3D-Net, we first render the input 3D shape  $m$  into  $V = 12$  views, where the viewpoints uniformly distribute on in a circle around the input shape. After the generally semantic part detection with  $S_R = 0.7$ , the features of top  $K = 20$  parts in each view are propagated to the hierarchical part-view attention aggregation module in Fig. 3 (d). In the view feature enhancement, the GRU cell [64] is adopted in our recurrent neural network and the dimension of the hidden state is initialized with 4,096. For all experiments, we train our network on a NVIDIA GTX 1,080Ti GPU using ADAM optimizer with an initial learning rate of 0.00001 and a batch size of 1.

### B. Parameter setting

There are several important hyperparameters in the setting of FG3D-Net. To investigate the influences of these hyperparameters, we have done some comparisons with different hyperparameters settings under the category of airplane, which contains 4,173 3D shapes from 13 subcategories. We first explore the number of input views  $V$  which determines the coverage of input 3D shapes from different view angles. In this experiment, we keep other hyperparameters fixed and only modifies the number of rendered views  $V$  from 3 to 12. The results are listed in TABLE III, where the instance accuracies increase with the number of views. And with  $V = 12$  views as input, FG3D-Net reaches the best accuracy of 93.99%. Considering the training time, we did not try more views.  $V = 12$  is also a widely used hyperparameter setting which have achieved satisfying performances in some related methods such as MVCNN [1], SeqViews2SeqLabels [13] and 3D2SeqViews [52].

TABLE III  
THE EFFECT OF THE VIEW NUMBER  $V$  ON THE PERFORMANCE IN FG3D-NET.

$V$	3	6	12
Acc (%)	88.39	92.90	<b>93.99</b>

In the following experiments, we keep the number of input views  $V = 12$ . In TABLE IV, we reveal the effect of the number  $K$  of generally semantic parts in the hierarchical part-view attention aggregation module in Fig. 3 (d). We range the number  $K$  of selected generally semantic parts from 5 to 40. The best accuracy 93.99% reaches at  $K = 20$ , which can

TABLE IV  
THE EFFECT OF THE NUMBER OF GENERALLY SEMANTIC PARTS  $K$  ON THE PERFORMANCE IN FG3D-NET.

$K$	5	10	20	30	40
Acc (%)	92.90	93.31	<b>93.99</b>	93.58	93.44

TABLE V  
THE EFFECT OF RNN CELL TYPES (CTs) ON THE PERFORMANCE IN FG3D-NET.

CT	BasicRNN	LSTM	BidirectionRNN	GRU
Acc (%)	91.80	92.76	93.44	<b>93.99</b>

achieve a better coverage of the fine-grained details of 3D shapes.

To investigate the effect of the RNN cell type (CT) in the *view feature enhancement*, we show the results with different RNN cells in TABLE V. From these results, the GRU cell outperforms other RNN cells such as BasicRNN, LSTM and BidirectionRNN. In particular, in the BidirectionRNN cell, there are two GRU cells of different directions.

TABLE VI  
THE EFFECT OF THE DIMENSION (Dim) OF GRU CELL ON THE PERFORMANCE.

Dim	512	1024	2048	4096	5120
Acc (%)	93.03	93.44	93.17	<b>93.99</b>	92.76

TABLE VII  
THE EFFECT OF THE ATTENTION MECHANISM ON THE PERFORMANCE UNDER AIRPLANE IN FG3D-NET.

Metric	OVA	OPA	NA	NR
Acc (%)	93.31	93.58	92.90	91.94

Moreover, we explore the effect of the RNN's hidden state dimension (Dim) which affects the learning ability of the recurrent neural network. As depicted in TABLE VI, the dimension of GRU cell is modified from 512 to 5,120. The best performance achieves at  $Dim = 4096$ , which can better capture the spatial correlation of sequential views.

### C. Ablation study

In order to reveal the effect of some novel elements in FG3D-Net, such as attention mechanisms in different semantic levels, we do some ablation studies to justify their effectiveness. We evaluate the performance of FG3D-Net with only part-level attention (OPA), only view-level attention (OVA), no attention (NA) or no RNN (NR). Specifically, when we remove the attention mechanism, we set all attention values to the same constant. For example, we set the part-level attention value to  $\frac{1}{20}$  in OVA and the view-level attention value  $\frac{1}{12}$  in OPA. TABLE VII illustrates the effectiveness of our attention mechanisms in learning high discriminative representations for 3D shapes. The results show that both part attention and view attention play an important role in extracting fine-grained details from multiple views. Without the RNN layer, the performance of FG3D-Net drops a lot. The possible reasons are the reduction of network parameters and

TABLE VIII  
THE SHAPE CLASSIFICATION ACCURACY(%) COMPARISON UNDER AIRPLANE, CHAIR AND CAR BENCHMARKS.

Method	Modality	Input	Airplane		Chair		Car	
			Class	Instance	Class	Instance	Class	Instance
PointNet[41]	point	$1024 \times 3$	82.67	89.34	72.07	75.44	68.12	73.00
PointNet++ [42]	point	$1024 \times 3$	87.26	92.21	78.11	80.78	70.30	75.21
SO-Net [65]	point	$1024 \times 3$	66.10	82.92	62.78	70.05	53.38	59.32
Point2Sequence [66]	point	$1024 \times 3$	87.52	92.76	74.90	79.12	64.67	73.54
VoxNet [67]	voxel	$32^3$	84.45	89.62	66.50	72.18	63.75	67.83
MVCNN [1]	view	$12 \times 224^2$	82.57	91.11	76.27	82.90	71.88	76.12
RotationNet [11]	view	$12 \times 224^2$	89.11	92.76	78.45	82.07	72.53	75.59
SeqViews2SeqLabels [13]	view	$12 \times 224^2$	88.52	93.44	79.89	82.54	72.23	75.36
Part4Feature [12]	view	$12 \times 224^2$	82.55	91.39	77.08	81.61	73.42	75.44
Ours	view	$12 \times 224^2$	<b>89.44</b>	<b>93.99</b>	<b>80.04</b>	<b>83.94</b>	<b>74.03</b>	<b>79.47</b>

the lack of spatial correlations among views. In other words, the spatial correlation among views is important for the fine-grained classification of 3D shapes.

#### D. Fine-grained visual classification

We carry out the experiments in the fine-grained classification of 3D shapes under the proposed FG3D dataset with three categories including *Airplane*, *Car* and *Chair*. In TABLE I, there are 4,173, 8,325 and 13,054 shapes in the categories, which are split into training set and testing set. To evaluate the performance of FG3D-Net, we compare our method with several state-of-the-art 3D shape classification methods which are trained under different 3D shape representations including point clouds, rendered views and 3D voxels. In TABLE VIII, the comparison methods include PointNet [41], PointNet++ [42], SO-Net [65], Point2Sequence [66], MVCNN [1] and Parts4Feature [12]. For these methods, we reproduce network structures using the public source code and evaluate them under our FG3D dataset.

In the comparison with other methods, we adopt MVCNN [1] as our baseline. MVCNN is the pioneer study in the recognition of 3D shapes from multiple views, which has achieved satisfactory performances in shape classification task. MVCNN leverages 12 views rendered around each 3D shape as input. We follow this setting of MVCNN and evaluate the performances of other view-based methods, including RotationNet [11], SeqViews2SeqLabels [13] and Parts4Feature [12]. RotationNet learns the best camera setting to capture the view-specific feature representation for 3D shapes, which has obtained superior performance to previous state-of-the-art methods under ModelNet40 and ModelNet10. Therefore, in this paper, we compare FG3D-Net with RotationNet under the FG3D dataset with the same input condition. To utilize the sequential views, SeqViews2SeqLabels adopts a recurrent neural network to aggregate multiple views of 3D shapes. However, SeqViews2SeqLabels can not explore the fine-grained information among GSPs extracted from the shape views. Parts4Feature is also a baseline of our FG3D-Net, which also detects generally semantic parts inside views. However, Parts4Feature cannot fully explore the fine-grained correlation among features at different semantic level, such as view-level. There is no view feature used in Part4Feature, which results in the lack of view-level information in the feature aggregation.

In addition, we also show the results of some methods that take other data formats as input under FG3D dataset. For point cloud based methods, we first choose the pioneer methods PointNet [41] and PointNet++ [42] as the comparison targets. We also do comparison with other state-of-the-art point cloud based methods including SO-Net [65] and Point2Sequence [66]. To translate our FG3D dataset into point clouds, we apply the Poisson Disk Sampling [68] to sample 1,024 points for each 3D shape. All point cloud based method are trained with 1,024 points as input under the FG3D dataset. VoxNet [67] also listed in the TABLE VIII, which is the pioneer work of voxel-based methods in 3D shape recognition.

As shown in TABLE VIII, our FG3D-Net outperforms other state-of-the-art methods and achieves highest classification accuracies in all three categories. The results suggest that FG3D-Net can take advantage of generally semantic part detection to integrate fine-grained details in multiple views. With a hierarchical aggregation strategy, we fully explore the correlation of features in different semantic levels.

## VI. VISUALIZATION

In this section, we reveal the visualizations of some important results in our FG3D-Net. Firstly, we show some examples of the detection of generally semantic parts under our FG3D testing set. In Fig. 8, we draw the bounding box of GSPs whose semantic score is larger than 0.8. From the results, FG3D-Net can extract the bounding box of discriminative GSPs which supports the representation learning of 3D shapes. And in our FG3D-Net, there are two important attention mechanisms including part-level attention and view-level attention. To learn the global representation of 3D shapes, these attention mechanisms are important to preserve the fine-grained details inside GSPs from multiple views. And in order to intuitively show the effectiveness of attentions, we respectively draw some samples of part-level attention in Fig. 9 and view-level attention in Fig. 10, respectively. In Fig. 9, we show the attention map  $q(k, k')$  of 9 views from 3 different categories. In each view, we draw the bounding boxes of top 20 GSPs, where the most discriminative GSPs with large attention values is in red. And we use arrows to indicate the correspondence of GSPs and attention values in the attention map  $q(k, k')$ , where each column represents the attention value of each GSP. Similar to the part-level attention, we visualize the view-level attention, as shown in Fig. 10. In Fig. 10, each row shows the



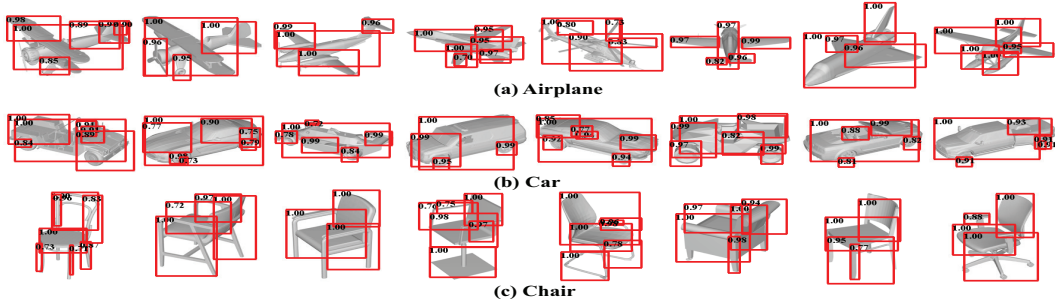


Fig. 8. The results of generally semantic part detection, where the semantic score of each part is larger than 0.8.

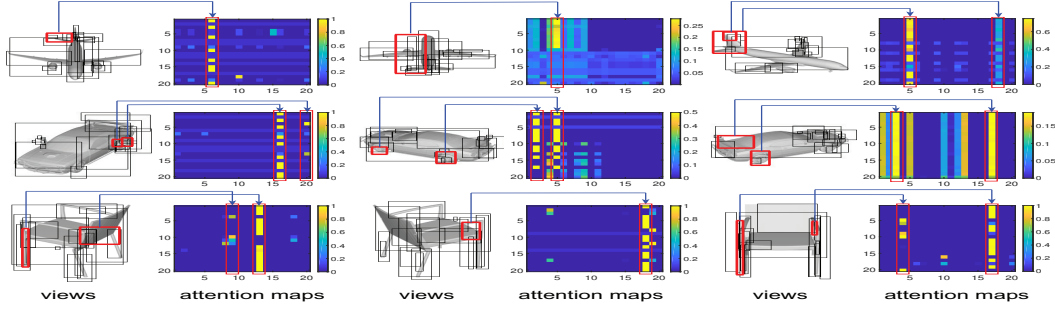


Fig. 9. The visualizations of the part-level attention. There are 9 views from the 3 categories of our FG3D dataset, where the top 20 GSPs are drawn in each image. The corresponding bilinear similarity attention map  $q(k, k')$  of among GSPs in each view is shown on the right of the view with a size of  $20 \times 20$ . We highlight the discriminative GSPs with red bounding boxes and use arrows to indicate the corresponding columns on the attention maps.

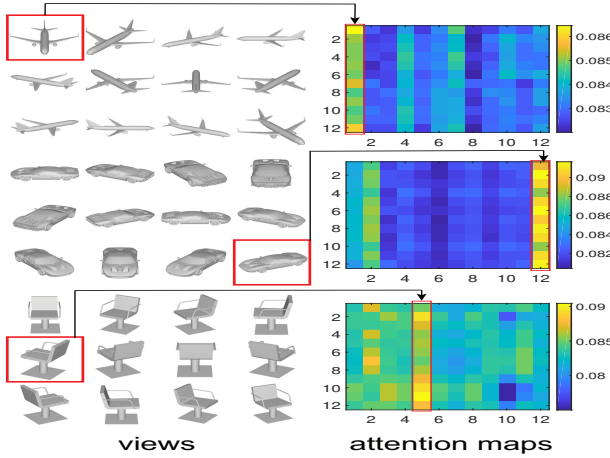


Fig. 10. The visualizations of the view-level attention. There are three 3D shapes selected from three different categories in our FG3D dataset. In each row, we show the 12 views of each 3D shape on the left and the attention map  $\theta(i, i')$  of the views with a size of  $12 \times 12$  on the right. We highlight the discriminative views with red bounding boxes and use arrows to indicate the corresponding columns on the attention maps.

12 views and the corresponding view attention map  $\theta(i, i')$  of a 3D shape. We also use arrows to indicate the correspondence of views and attention values on the attention maps. The visualization results show that both part-level attention and view-level attention are effective to capture the fine-grained information in the feature aggregation.

## VII. CONCLUSIONS AND FUTURE WORK

In this paper, we propose a novel deep learning model named FG3D-Net to learn 3D global features via hierarchically feature aggregation from GSPs. And to evaluate the performance of FG3D-Net, we introduce a new 3D fine-grained classification dataset. In existing methods, the fine-grained details of generally semantic parts and the correlation of features in different semantic levels are usually ignored, which limits the discriminativeness of learned 3D global features in the fine-grained 3D shape classification. To resolve these disadvantages, FG3D-Net employs a region proposal neural network to detect GSPs from multiple views, which searches out discriminative local parts inside views to learn the fine-grained details of 3D shapes. In addition, the part-level attention and the view-level attention learn to effectively aggregate features in different semantic levels, which utilize the correlations among features to highlight the discriminative features. Finally, a recurrent neural network is adopted to capture the spatial information among views from multiple viewpoints, which takes advantage of the prior information of sequential views. Experimental results show that our method outperforms the state-of-the-art under the proposed 3D fine-grained dataset.

Although FG3D-Net learns 3D shape global features from GSPs with high performances, it still suffers from two limitations. First, FG3D-Net can only detect the GSPs learned from segmentation benchmarks rather than the most suitable GSPs from the FG3D dataset. Second, the number of categories in our FG3D dataset is still limited, where only three categories are included in our dataset. Thus, FG3D-Net merely performs

well under current input setting and limited number of 3D shapes, even with the help of bilinear similarity attention and RNN. In the future, it is worth to explore some unsupervised methods to detect GSPs inside multiple views and to further refine our FG3D dataset.

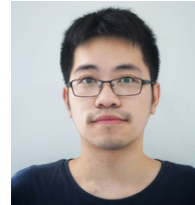
## REFERENCES

- [1] H. Su, S. Maji, E. Kalogerakis, and E. Learned-Miller, "Multi-view convolutional neural networks for 3D shape recognition," in *IEEE International Conference on Computer Vision*, 2015.
- [2] S. Bai, X. Bai, Z. Zhou, Z. Zhang, Q. Tian, and L. J. Latecki, "GIFT: Towards scalable 3D shape retrieval," *IEEE Transactions on Multimedia*, vol. 19, no. 6, pp. 1257–1271, 2017.
- [3] A. Kanezaki, Y. Matsushita, and Y. Nishida, "RotationNet: Joint object categorization and pose estimation using multiviews from unsupervised viewpoints," in *IEEE Conference on Computer Vision and Pattern Recognition*, 2018.
- [4] Z. Han, M. Shang, X. Wang, Y.-S. Liu, and M. Zwicker, "Y2Seq2Seq: Cross-modal representation learning for 3D shape and text by joint reconstruction and prediction of view and word sequences," in *AAAI Conference on Artificial Intelligence*, vol. 33, 2019, pp. 126–133.
- [5] J. Deng, W. Dong, R. Socher, L.-J. Li, K. Li, and L. Fei-Fei, "ImageNet: A large-scale hierarchical image database," in *IEEE Conference on Computer Vision and Pattern Recognition*. IEEE, 2009, pp. 248–255.
- [6] S. Ren, K. He, R. Girshick, and J. Sun, "Faster R-CNN: Towards real-time object detection with region proposal networks," in *Advances in Neural Information Processing Systems*, 2015, pp. 91–99.
- [7] C. Wah, S. Branson, P. Welinder, P. Perona, and S. Belongie, "The caltech-UCSD birds-200-2011 dataset," 2011.
- [8] A. Khosla, N. Jayadevaprakash, B. Yao, and F.-F. Li, "Novel dataset for fine-grained image categorization: Stanford dogs," in *Proc. CVPR Workshop on Fine-Grained Visual Categorization*, vol. 2, no. 1, 2011.
- [9] A. X. Chang, T. Funkhouser, L. Guibas, P. Hanrahan, Q. Huang, Z. Li, S. Savarese, M. Savva, S. Song, H. Su *et al.*, "ShapeNet: An information-rich 3D model repository," *Technical Report arXiv:1512.03012*, 2015.
- [10] P. Shilane, P. Min, M. Kazhdan, and T. Funkhouser, "The Princeton shape benchmark," in *Shape Modeling Applications*. IEEE, 2004, pp. 167–178.
- [11] A. Kanezaki, Y. Matsushita, and Y. Nishida, "RotationNet: Joint object categorization and pose estimation using multiviews from unsupervised viewpoints," in *IEEE Conference on Computer Vision and Pattern Recognition*, 2018, pp. 5010–5019.
- [12] Z. Han, X. Liu, Y.-S. Liu, and M. Zwicker, "Parts4Feature: Learning 3D global features from generally semantic parts in multiple views," *International Joint Conference on Artificial Intelligence*, 2019.
- [13] Z. Han, M. Shang, Z. Liu, C.-M. Vong, Y.-S. Liu, M. Zwicker, J. Han, and C. P. Chen, "SeqViews2SeqLabels: Learning 3D global features via aggregating sequential views by RNN with attention," *IEEE Transactions on Image Processing*, vol. 28, no. 2, pp. 658–672, 2018.
- [14] G. A. Miller, "WordNet: A lexical database for English," *Communications of the ACM*, vol. 38, no. 11, pp. 39–41, 1995.
- [15] S. Seok, C. D. Onal, K.-J. Cho, R. J. Wood, D. Rus, and S. Kim, "MeshWorm: A peristaltic soft robot with antagonistic nickel titanium coil actuators," *IEEE/ASME Transactions on Mechatronics*, vol. 18, no. 5, pp. 1485–1497, 2012.
- [16] N. Wang, Y. Zhang, Z. Li, Y. Fu, W. Liu, and Y.-G. Jiang, "Pixel2Mesh: Generating 3D mesh models from single RGB images," in *European Conference on Computer Vision*, 2018, pp. 52–67.
- [17] F. Bogo, J. Romero, M. Loper, and M. J. Black, "FAUST: Dataset and evaluation for 3D mesh registration," in *IEEE Conference on Computer Vision and Pattern Recognition*, 2014, pp. 3794–3801.
- [18] A. M. Bronstein, M. M. Bronstein, and R. Kimmel, *Numerical geometry of non-rigid shapes*. Springer Science & Business Media, 2008.
- [19] S. Koch, A. Matveev, Z. Jiang, F. Williams, A. Artemov, E. Burnaev, M. Alexa, D. Zorin, and D. Panozzo, "ABC: A big CAD model dataset for geometric deep learning," in *IEEE Conference on Computer Vision and Pattern Recognition*, 2019, pp. 9601–9611.
- [20] H. Benhabiles, J.-P. Vandeboer, G. Lavoué, and M. Daoudi, "A framework for the objective evaluation of segmentation algorithms using a ground-truth of human segmented 3D-models," in *IEEE International Conference on Shape Modeling and Applications*. IEEE, 2009, pp. 36–43.
- [21] R. Hu, L. Fan, and L. Liu, "Co-segmentation of 3D shapes via subspace clustering," in *Computer Graphics Forum*, vol. 31, no. 5. Wiley Online Library, 2012, pp. 1703–1713.
- [22] E. Kalogerakis, A. Hertzmann, and K. Singh, "Learning 3D mesh segmentation and labeling," in *ACM Transactions on Graphics*, vol. 29, no. 4. ACM, 2010, p. 102.
- [23] Y. Wang, S. Asafi, O. Van Kaick, H. Zhang, D. Cohen-Or, and B. Chen, "Active co-analysis of a set of shapes," *ACM Transactions on Graphics*, vol. 31, no. 6, p. 165, 2012.
- [24] K. Mo, S. Zhu, A. X. Chang, L. Yi, S. Tripathi, L. J. Guibas, and H. Su, "PartNet: A large-scale benchmark for fine-grained and hierarchical part-level 3D object understanding," in *IEEE Conference on Computer Vision and Pattern Recognition*, 2019, pp. 909–918.
- [25] S. Maji, E. Rahtu, J. Kannala, M. Blaschko, and A. Vedaldi, "Fine-grained visual classification of aircraft," *Technical Report arXiv:1306.5151*, 2013.
- [26] J. Krause, M. Stark, J. Deng, and L. Fei-Fei, "3D object representations for fine-grained categorization," in *International IEEE Workshop on 3D Representation and Recognition*, Sydney, Australia, 2013.
- [27] D. Wang, Z. Shen, J. Shao, W. Zhang, X. Xue, and Z. Zhang, "Multiple granularity descriptors for fine-grained categorization," in *IEEE International Conference on Computer Vision*, 2015, pp. 2399–2406.
- [28] T.-Y. Lin, A. RoyChowdhury, and S. Maji, "Bilinear CNN models for fine-grained visual recognition," in *IEEE International Conference on Computer Vision*, 2015, pp. 1449–1457.
- [29] M. Jaderberg, K. Simonyan, A. Zisserman *et al.*, "Spatial transformer networks," in *Advances in Neural Information Processing Systems*, 2015, pp. 2017–2025.
- [30] P. Sermanet, A. Frome, and E. Real, "Attention for fine-grained categorization," *International Conference on Learning Representations Workshop*, 2015.
- [31] N. Zhang, J. Donahue, R. Girshick, and T. Darrell, "Part-based R-CNNs for fine-grained category detection," in *European Conference on Computer Vision*. Springer, 2014, pp. 834–849.
- [32] M. Simon and E. Rodner, "Neural activation constellations: Unsupervised part model discovery with convolutional networks," in *IEEE International Conference on Computer Vision*, 2015, pp. 1143–1151.
- [33] Y. Zhang, X.-S. Wei, J. Wu, J. Cai, J. Lu, V.-A. Nguyen, and M. N. Do, "Weakly supervised fine-grained categorization with part-based image representation," *IEEE Transactions on Image Processing*, vol. 25, no. 4, pp. 1713–1725, 2016.
- [34] Z. Han, Z. Liu, J. Han, C.-M. Vong, S. Bu, and X. Li, "Unsupervised 3D local feature learning by circle convolutional restricted Boltzmann machine," *IEEE Transactions on Image Processing*, vol. 25, no. 11, pp. 5331–5344, 2016.
- [35] Z. Han, Z. Liu, J. Han, C.-M. Vong, S. Bu, and C. L. P. Chen, "Mesh convolutional restricted Boltzmann machines for unsupervised learning of features with structure preservation on 3D meshes," *IEEE Transactions on Neural Networks and Learning Systems*, vol. 28, no. 10, pp. 2268–2281, 2016.
- [36] Z. Wu, S. Song, A. Khosla, F. Yu, L. Zhang, X. Tang, and J. Xiao, "3d ShapeNets: A deep representation for volumetric shapes," in *IEEE Conference on Computer Vision and Pattern Recognition*, 2015, pp. 1912–1920.
- [37] A. Sharma, O. Grau, and M. Fritz, "VConv-DAE: Deep volumetric shape learning without object labels," in *European Conference on Computer Vision (ECCV)*. Springer, 2016, pp. 236–250.
- [38] C. R. Qi, H. Su, M. Nießner, A. Dai, M. Yan, and L. J. Guibas, "Volumetric and multi-view cnns for object classification on 3D data," in *IEEE Conference on Computer Vision and Pattern Recognition*, 2016, pp. 5648–5656.
- [39] J. Wu, C. Zhang, T. Xue, B. Freeman, and J. Tenenbaum, "Learning a probabilistic latent space of object shapes via 3D generative-adversarial modeling," in *Advances in Neural Information Processing Systems*, 2016, pp. 82–90.
- [40] S. Muralikrishnan, V. G. Kim, and S. Chaudhuri, "Tags2Parts: Discovering semantic regions from shape tags," in *IEEE Conference on Computer Vision and Pattern Recognition*, 2018, pp. 2926–2935.
- [41] C. R. Qi, H. Su, K. Mo, and L. J. Guibas, "PointNet: Deep learning on point sets for 3D classification and segmentation," in *IEEE Conference on Computer Vision and Pattern Recognition*, 2017, pp. 652–660.
- [42] C. R. Qi, L. Yi, H. Su, and L. J. Guibas, "PointNet++: Deep hierarchical feature learning on point sets in a metric space," in *Advances in Neural Information Processing Systems*, 2017, pp. 5099–5108.
- [43] Y. Yang, C. Feng, Y. Shen, and D. Tian, "FoldingNet: Point cloud auto-encoder via deep grid deformation," in *IEEE Conference on Computer Vision and Pattern Recognition*, 2018, pp. 206–215.

- [44] P. Achlioptas, O. Diamanti, I. Mitliagkas, and L. Guibas, "Learning representations and generative models for 3D point clouds," in *International Conference on Machine Learning*, 2018, pp. 40–49.
- [45] Z. Han, X. Wang, Y.-S. Liu, and M. Zwicker, "Multi-angle point cloud-VAE: Unsupervised feature learning for 3D point clouds from multiple angles by joint self-reconstruction and half-to-half prediction," in *IEEE International Conference on Computer Vision*, October 2019.
- [46] Z. Han, M. Shang, Y.-S. Liu, and M. Zwicker, "View inter-prediction GAN: Unsupervised representation learning for 3D shapes by learning global shape memories to support local view predictions," in *AAAI Conference on Artificial Intelligence*, vol. 33, 2019, pp. 8376–8384.
- [47] B. Shi, S. Bai, Z. Zhou, and X. Bai, "DeepPano: Deep panoramic representation for 3D shape recognition," *IEEE Signal Processing Letters*, vol. 22, no. 12, pp. 2339–2343, 2015.
- [48] K. Sfikas, T. Theoharis, and I. Pratikakis, "Exploiting the PANORAMA representation for convolutional neural network classification and retrieval," *3DOR*, vol. 6, p. 7, 2017.
- [49] H. Su, S. Maji, E. Kalogerakis, and E. Learned-Miller, "Multi-view convolutional neural networks for 3D shape recognition," in *IEEE International Conference on Computer Vision*, 2015, pp. 945–953.
- [50] E. Johns, S. Leutenegger, and A. J. Davison, "Pairwise decomposition of image sequences for active multi-view recognition," in *IEEE Conference on Computer Vision and Pattern Recognition*, 2016, pp. 3813–3822.
- [51] C. Wang, M. Pelillo, and K. Siddiqi, "Dominant set clustering and pooling for multi-view 3D object recognition," *British Machine Vision Conference*, 2017.
- [52] Z. Han, H. Lu, Z. Liu, C.-M. Vong, Y.-S. Liua, M. Zwicker, J. Han, and C. P. Chen, "3D2SeqViews: Aggregating sequential views for 3D global feature learning by CNN with hierarchical attention aggregation," *IEEE Transactions on Image Processing*, 2019.
- [53] C. Goldfeder and P. Allen, "Autotagging to improve text search for 3D models," in *ACM/IEEE-CS Joint Conference on Digital Libraries*. ACM, 2008, pp. 355–358.
- [54] "Yobi3D - Free 3D model search engine," <https://www.yobi3d.com>, Accessed: 2019-12-11.
- [55] K. Simonyan and A. Zisserman, "Very deep convolutional networks for large-scale image recognition," in *International Conference on Learning Representations*, 2015.
- [56] L. Yi, V. G. Kim, D. Ceylan, I. Shen, M. Yan, H. Su, C. Lu, Q. Huang, A. Sheffer, L. Guibas *et al.*, "A scalable active framework for region annotation in 3D shape collections," *ACM Transactions on Graphics*, vol. 35, no. 6, p. 210, 2016.
- [57] X. Chen, A. Golovinskiy, and T. Funkhouser, "A benchmark for 3D mesh segmentation," in *ACM Transactions on Graphics*, vol. 28, no. 3, ACM, 2009, p. 73.
- [58] E. Kalogerakis, M. Averkiou, S. Maji, and S. Chaudhuri, "3d shape segmentation with projective convolutional networks," in *IEEE Conference on Computer Vision and Pattern Recognition*, 2017, pp. 3779–3788.
- [59] R. Girshick, J. Donahue, T. Darrell, and J. Malik, "Rich feature hierarchies for accurate object detection and semantic segmentation," in *IEEE Conference on Computer Vision and Pattern Recognition*, 2014, pp. 580–587.
- [60] H. Zheng, J. Fu, T. Mei, and J. Luo, "Learning multi-attention convolutional neural network for fine-grained image recognition," in *IEEE International Conference on Computer Vision*, 2017, pp. 5209–5217.
- [61] Z. Wang, T. Chen, G. Li, R. Xu, and L. Lin, "Multi-label image recognition by recurrently discovering attentional regions," in *IEEE International Conference on Computer Vision*, 2017, pp. 464–472.
- [62] P. Guo and R. Farrell, "Aligned to the object, not to the image: A unified pose-aligned representation for fine-grained recognition," in *IEEE Winter Conference on Applications of Computer Vision*. IEEE, 2019, pp. 1876–1885.
- [63] W. Ge, X. Lin, and Y. Yu, "Weakly supervised complementary parts models for fine-grained image classification from the bottom up," in *IEEE Conference on Computer Vision and Pattern Recognition*, 2019, pp. 3034–3043.
- [64] K. Cho, B. van Merriënboer, C. Gulcehre, D. Bahdanau, F. Bougares, H. Schwenk, and Y. Bengio, "Learning phrase representations using RNN Encoder-Decoder for statistical machine translation," in *Conference on Empirical Methods in Natural Language Processing*. Association for Computational Linguistics, 2014, pp. 1724–1734.
- [65] J. Li, B. M. Chen, and G. Hee Lee, "SO-Net: Self-organizing network for point cloud analysis," in *IEEE Conference on Computer Vision and Pattern Recognition*, 2018, pp. 9397–9406.
- [66] X. Liu, Z. Han, Y.-S. Liu, and M. Zwicker, "Point2Sequence: Learning the shape representation of 3D point clouds with an attention-based

sequence to sequence network," in *AAAI Conference on Artificial Intelligence*, vol. 33, 2019, pp. 8778–8785.

- [67] D. Maturana and S. Scherer, "VoxNet: A 3D convolutional neural network for real-time object recognition," in *IEEE/RSJ International Conference on Intelligent Robots and Systems*. IEEE, 2015, pp. 922–928.
- [68] C. Feng, "Cython wrapper of poisson disk sampling of a triangle mesh in vcglib," <https://github.com/simbaforsrest/trimesh2pointcloud>, Last accessed: 2020-01-12.



**Xinhai Liu** received the B.S. degree in computer science and technology from the Huazhong University of Science and Technology, China, in 2017. He is currently the PhD student with the School of Software, Tsinghua University. His research interests include deep learning, 3D shape analysis and 3D pattern recognition.



**Zhizhong Han** received the Ph.D. degree from Northwestern Polytechnical University, China, 2017. He is currently a Post-Doctoral Researcher with the Department of Computer Science, University of Maryland at College Park, College Park, USA. He is also a Research Member of the BIM Group, Tsinghua University, China. His research interests include machine learning, pattern recognition, feature learning, and digital geometry processing.



**Yu-Shen Liu** (M'18) received the B.S. degree in mathematics from Jilin University, China, in 2000, and the Ph.D. degree from the Department of Computer Science and Technology, Tsinghua University, Beijing, China, in 2006. From 2006 to 2009, he was a Post-Doctoral Researcher with Purdue University. He is currently an Associate Professor with the School of Software, Tsinghua University. His research interests include shape analysis, pattern recognition, machine learning, and semantic search.



**Matthias Zwicker** is a professor at the Department of Computer Science, University of Maryland, College Park, where he holds the Reginald Allan Hahne Endowed E-nnovate chair. He obtained his PhD from ETH in Zurich, Switzerland, in 2003. Before joining University of Maryland, he was an Assistant Professor at the University of California, San Diego, and a professor at the University of Bern, Switzerland. His research in computer graphics covers signal processing for high-quality rendering, point-based methods for rendering and modeling, 3D geometry processing, and data-driven modeling and animation.